A Numerical Study of Steady Pollutant Spread in Water from a Point Source

Nurcahya Yulian Ashar, Imam Solekhudin*

***Abstract*—In this paper, problems involving steady pollutant spread from a point source in a path with laminar water flow are studied. Three different paths with different inclination angles are considered. The problems are governed by diffusion-convection equations. These governing equations may not be solved analytically. Hence, in this paper a numerical method called Dual Reciprocity Method (DRM) is employed to solve the problems numerically. The numerical solutions are presented to determine the effect or influence of inclination angles to the pollutant concentration in the water.**

***Index Terms*—Dual reciprocity method, diffution-convection equation, velocity profile, Navier-Stokes equation, laminar flow.**

I. Introduction

DIFFUSION-convection equation is widely used to modelled problems involving pollution spread in fluid path. One of the purposes of modelling the problems mathematically is to study the problems more efficiently. To study the problems mathematically, derivation of mathematical models is needed. One of such derivation is presented by Samec [1]. Resulting mathematical models of these problems are then solved to obtain required solutions. To solve the problems, analytical and numerical methods are used. Some of analytical studies of diffusion-convection problems have been conducted by Polyanin [2] and Morales-Delgadoa et. al. [3]. However, analytical methods may only be applied for limited number of problems.

Most of the resulting mathematical models may not be solved analytically. Hence numerical methods are employed to solve the mathematical models. Some of numerical studies of diffusion-convection problems have been conducted by numerous researchers. Such researchers are Fajie et. al. [4], Xingxing et. al. [5], Mengxing et. al. [6], and [7]. In these numerical studies, problems with point sources has not been considered.

To incorporate point sources into the problems, one of suitable method is Dual Reciprocity Method (DRM), which is part of Boundary Element Methods (BEM). These methods, BEM and DRM, have been used by researchers to solve various problems. Such researchers are Clements and Lobo [8], Solekhudin and Ang [9], Solekhudin [10], Munadi et. al. [11], Yun and Ang [12], and Ashar [13]. Researchers in [8], [9], [10], and [11] studied water infiltration from irrigation channels into soils. Yun and Ang studied heat conduction in non-homogeneous solid [12]. Ashar studied pollutant spread in a river [13]. DRM has been reported for its flexibility. Moreover, DRM may be employed to solve problems over any domain shape bounded by a simple closed curve. In this paper, a DRM is used to solve pollutant spread from a point source over shallow fluid paths with different inclinations. Some numerical solutions obtained are presented to investigate the influence of inclination to distribution of pollutant concentration over the shallow fluid paths.

Manuscript received September 21, 2020; revised April 27, 2021.

Nurcahya Yulian Ashar is an M.Sc. student at Department of Mathematics, Faculty of Mathematics and Natural Sciences, Universitas Gadjah Mada, Yogyakarta, INDONESIA. Email: nurcahyayulian@gmail.com

*Corresponding author. Imam Solekhudin is an Associate Professor at Department of Mathematics, Faculty of Mathematics and Natural Sciences, Universitas Gadjah Mada, Yogyakarta, INDONESIA. Email: imams@ugm.ac.id

II. Problem formulation and basic equations

In this section, the mathematical model of steady diffusion-convection problems is presented. A brief derivation of DRM for solving the problems is also presented. Steady diffusion-convection problems over a region Ω bounded by simple closed curve Γ are governed by

$$f_1\frac{\partial T}{\partial x}+f_2\frac{\partial T}{\partial y}-D\left(\frac{\partial^2 T}{\partial x^2}+\frac{\partial^2 T}{\partial y^2}\right)=Q(x,y), \quad (1)$$

where T is pollutant concentration, f_1 and f_2 are fluid velocity in x and y direction respectively, D is pollutant diffution coefficient in fluid, and Q is the source. For problems with a point source, the governing equation is

$$f_1\frac{\partial T}{\partial x}+f_2\frac{\partial T}{\partial y}-D\left(\frac{\partial^2 T}{\partial x^2}+\frac{\partial^2 T}{\partial y^2}\right) = Q(x,y)\sigma(x,y;a,b), \quad (2)$$

where (a,b) is the coordinate of the source, and σ is a Dirac delta function with the source at (a,b). Equation (1) and (2) may be solved numerically using DRM. To solve Equation (1) and (2) using DRM, we first express their solutions in the form of boundary integral equations. The boundary integral equations for Equations (1) and (2) are

$$\begin{aligned}\lambda(\alpha,\beta)\,T(\alpha,\beta) = & \int_\Gamma\left[T(x,y)\frac{\partial\Phi(x,y;\alpha,\beta)}{\partial n}-\Phi(x,y;\alpha,\beta)\frac{\partial T(x,y)}{\partial n}\right]ds + \\ & \frac{1}{D}\iint_\Omega \Phi(x,y;\alpha,\beta)\left[f_1(x,y)\frac{\partial T(x,y)}{\partial x}+f_2(x,y)\frac{\partial T(x,y)}{\partial y}-Q(x,y)\right]dx\,dy, \end{aligned} \quad (3)$$

and

$$\begin{aligned}\lambda(\alpha,\beta)T(\alpha,\beta) &= \int_\Gamma \left[T(x,y)\frac{\partial\Phi(x,y;\alpha,\beta)}{\partial n} - \Phi(x,y;\alpha,\beta)\frac{\partial T(x,y)}{\partial n}\right]ds + \\ &\frac{1}{D}\iint_\Omega \Phi(x,y;\alpha,\beta)\left[f_1(x,y)\frac{\partial T(x,y)}{\partial x} + f_2(x,y)\frac{\partial T(x,y)}{\partial y}\right]dx\,dy - \\ &\frac{\Phi(x,y;\alpha,\beta)Q(x,y)}{D}, \qquad (4)\end{aligned}$$

respectively. Here

$$\lambda(\alpha,\beta) = \begin{cases} 1 & ,(\alpha,\beta)\in\Omega \\ \frac{1}{2} & ,(\alpha,\beta) \text{ on the smooth part of } \Gamma, \end{cases}$$

and

$$\Phi(x,y;\alpha,\beta) = \frac{1}{4\pi}\ln\left[(x-\alpha)^2+(y-\beta)^2\right]$$

is the fundamental solution of two-dimensional Laplace's equation. From integral Equations (3) and (4), two systems of linear algebraic equations

$$\begin{aligned}\lambda^{(n)}T^{(n)} &= \sum_{k=1}^{N}\left[T^{(n)}\int_{\Gamma^{(k)}}\frac{\partial\Phi\left(x,y;x^{(n)},y^{(n)}\right)}{\partial n}ds - T_n^{(k)}\int_{\Gamma^{(k)}}\Phi\left(x,y;x^{(n)},y^{(n)}\right)ds\right] + \\ &\sum_{i=1}^{N+L}\left[f_1^{(n)}\mu_x^{(ni)} + f_2^{(n)}\mu_y^{(ni)}\right]T^{(i)} - \\ &\sum_{i=1}^{N+L}\mu^{(ni)}Q(x^{(i)},y^{(i)}) \\ &n = 1,2,\ldots,N+L, \qquad (5)\end{aligned}$$

and

$$\begin{aligned}\lambda^{(n)}T^{(n)} &= \sum_{k=1}^{N}\left[T^{(n)}\int_{\Gamma^{(k)}}\frac{\partial\Phi\left(x,y;x^{(n)},y^{(n)}\right)}{\partial n}ds - T_n^{(k)}\int_{\Gamma^{(k)}}\Phi\left(x,y;x^{(n)},y^{(n)}\right)ds\right] + \\ &\sum_{i=1}^{N+L}\left[f_1^{(n)}\mu_x^{(ni)} + f_2^{(n)}\mu_y^{(ni)}\right]T^{(i)} - \\ &\Phi(a,b;x^{(n)},y^{(n)})Q(a,b), \\ &n = 1,2,\ldots,N+L, \qquad (6)\end{aligned}$$

are respectively derived. Here N is the number of segment or element on boundary Γ, $\Gamma^{(1)}$, $\Gamma^{(2)}$,..., $\Gamma^{(N)}$ are the segments satisfy $\Gamma = \Gamma^{(1)}\cup\Gamma^{(2)}\cup\cdots\cup\Gamma^{(N)}$. Number L is the number of interior collocation point. Points $(x^{(1)},y^{(1)})$, $(x^{(2)},y^{(2)})$, ..., $(x^{(N)},y^{(N)})$ are the midpoints of segments $\Gamma^{(1)}$, $\Gamma^{(2)}$,..., $\Gamma^{(N)}$, respectively. Points $(x^{(N+1)},y^{(N+1)})$, $(x^{(N+2)},y^{(N+2)})$,...,$(x^{(N+L)},y^{(N+L)})$, are the interior collocation points,

$$\begin{aligned}\lambda^{(n)} &= \lambda(x^{(n)},y^{(n)}), \\ T^{(n)} &= T(x^{(n)},y^{(n)}), \\ T_n^{(n)} &= \left.\frac{\partial T(x,y)}{\partial n}\right|_{(x,y)=\left(x^{(n)},y^{(n)}\right)}, \\ f_1^{(n)} &= f_1(x^{(n)},y^{(n)}), \\ f_2^{(n)} &= f_2(x^{(n)},y^{(n)}),\end{aligned}$$

and

$$\begin{aligned}\mu_x^{(ni)} &= \sum_{j=1}^{N+L}\mu^{(ni)}\left.\frac{\partial\rho\left(x,y;x^{(j)},y^{(j)}\right)}{\partial x}\right|_{(x,y)=\left(x^{(i)},y^{(i)}\right)} \times \\ &\rho^{-1}\left(x^{(i)},y^{(i)};x^{(j)},y^{(j)}\right), \\ \mu_y^{(ni)} &= \sum_{j=1}^{N+L}\mu^{(ni)}\left.\frac{\partial\rho\left(x,y;x^{(j)},y^{(j)}\right)}{\partial y}\right|_{(x,y)=\left(x^{(i)},y^{(i)}\right)} \times \\ &\rho^{-1}\left(x^{(i)},y^{(i)};x^{(j)},y^{(j)}\right), \\ \mu^{(ni)} &= \sum_{j=1}^{N+L}\Psi^{(nj)}\rho^{-(ij)},\end{aligned}$$

$$\begin{aligned}\Psi^{(nj)} &= \lambda(x^{(n)},y^{(n)})\chi\left(x^{(n)},y^{(n)};x^{(j)},y^{(j)}\right) + \\ &\int_C\left[\Phi\left(x,y;x^{(n)},y^{(n)}\right)\frac{\partial\chi\left(x,y;x^{(j)},y^{(j)}\right)}{\partial n} - \chi\left(x,y;x^{(j)},y^{(j)}\right)\frac{\partial\Phi\left(x,y;x^{(n)},y^{(n)}\right)}{\partial n}\right]ds.\end{aligned}$$

Where

$$\rho^{(kl)} = 1 + r^2(x^{(k)},y^{(k)};x^{(l)},y^{(l)}) + r^3(x^{(k)},y^{(k)};x^{(l)},y^{(l)}),$$

and

$$\begin{aligned}\chi\left(x,y;x^{(m)},y^{(m)}\right) &= \frac{1}{4}r^2\left(x,y;x^{(m)},y^{(m)}\right) + \\ &\frac{1}{16}r^4\left(x,y;x^{(m)},y^{(m)}\right) + \\ &\frac{1}{25}r^5\left(x,y;x^{(m)},y^{(m)}\right).\end{aligned}$$

Function r is defined as

$$r(x,y;a,b) = \sqrt{(x-a)^2+(y-b)^2}.$$

By solving system of linear algebraic Equations (5) and (6), numerical solutions at collocation points may be obtained. Using these solutions, numerical solution at any $(\xi,\eta)\in\Omega\cup\Gamma$ may also be obtained.

III. Result and discussion

In this section, the DRM presented in Section II is applied to solve problems involving diffusion-convection equations. The first problem is a problem with analytical solution. This problem is used to investigate the accuracy of the DRM. The second problem is problem without analytical solution. This problem involving steady pollutant concentration range over shallow fluid path with a point source.

A. A Problem with analytic solution

We consider a problem involving diffusion-convection equation

$$g(x,y) = f_1(x,y)\frac{\partial T(x,y)}{\partial x} + f_2(x,y)\frac{\partial T(x,y)}{\partial y} - D\left(\frac{\partial^2 T(x,y)}{\partial x^2} + \frac{\partial^2 T(x,y)}{\partial y^2}\right) \quad (7)$$

with

$$f_1(x,y) = y,\ f_2(x,y) = x,\ D = 1,$$

and

$$g(x,y) = 2xy^3 + 2x^3y - 2x^2 - 2y^2,$$

defined over a square region with boundary conditions presented in Figure 1.

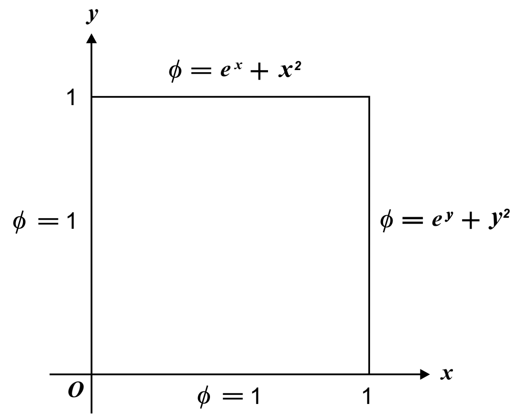

Fig. 1: Region and boundary conditions of diffusion-convection equation (7)

Analytical solution of Equation (7) subject to boundary conditions in Figure 1 is

$$\phi(x,y) = e^{xy} + x^2y^2.$$

To solve the problem using DRM, a number of element and interior point are needed. We consider two sets of element and interior points, namely Set A and Set B. In Set A, the number of elements is 80 and the number of interior collocation points is 81. In Set B, the number of elements and interior collocation points are 200 and 196, respectively. Absolute errors obtained using Set A and Set B are deninted by e_A and e_B. Some of the numerical results are presented in Table 1.

Table I shows numerical solutions at selected points obtained using the DRM with Set A and Set B. The corresponding analytical solutions and absolute errors are also presented in the table. It can be seen that numerical solutions obtained using the DRM are good in accuracy. It seems that the absolute errors of the numerical solutions obtained using Set A and Set B are less than 0.0006 and 0.0002, respectively. It can also be seen that Set B results in better accuracy than Set A. This means that generally the higher the number of segments and interior colllocation points the more accurate the numerical solution obtained.

TABLE I: Numerical and analytical solutions at selected points

Point	Analytic	Set A	Set B	e_A	e_B
$(0.2, 0.2)$	1.0424	1.04242	1.04241	0.000018	0.000005
$(0.4, 0.2)$	1.0896	1.08969	1.08970	0.000008	0.000013
$(0.6, 0.2)$	1.1418	1.14196	1.14192	0.000063	0.000028
$(0.8, 0.2)$	1.1991	1.19932	1.19917	0.000216	0.000061
$(0.2, 0.4)$	1.0896	1.08973	1.08969	0.000047	0.000003
$(0.4, 0.4)$	1.1991	1.19916	1.19912	0.000053	0.000014
$(0.6, 0.4)$	1.3288	1.32902	1.32889	0.000178	0.000047
$(0.8, 0.4)$	1.4795	1.48000	1.47964	0.000475	0.000119
$(0.2, 0.6)$	1.1418	1.14191	1.14189	0.000016	0.000006
$(0.4, 0.6)$	1.3288	1.32883	1.32884	0.000012	0.000007
$(0.6, 0.6)$	1.5629	1.56304	1.56295	0.000117	0.000028
$(0.8, 0.6)$	1.8464	1.84703	1.84661	0.000560	0.000143
$(0.2, 0.8)$	1.1991	1.19903	1.19908	0.000077	0.000026
$(0.4, 0.8)$	1.4795	1.47930	1.47946	0.000221	0.000060
$(0.6, 0.8)$	1.8464	1.84621	1.84640	0.000258	0.000071
$(0.8, 0.8)$	2.3060	2.30623	2.30611	0.000153	0.000036

B. Steady pollutant concentration in fluid paths with one point source

In this part, we apply the DRM to solve the steady pollutant concentration range in twinned fluid path with point source. We are given shallow path of water with the width of 24 m. To investigate the influence of inclination to pollutant concentration, the three cases are 30 $\deg$, 60 $\deg$, and 90 $\deg$ cases. For convenience, the three cases are denoted by Case 1, Case 2, and Case 3, respectively. A source with concentration of 200/107 gram/s and D=11.75 m^2/s is placed at point (24,24). The problem described is illustrated in Figure 2.

In Figure 2, a path which has width of 24 m is selected, provided that the boundary condition at the upstream is $T = 0$, and on the other part of the boundary is $\partial T/\partial n = 0$. Before computing numerical values of pollutant concentration using the DRM, laminar velocity profiles of water flow at interior collocation points need to be obtained. In this paper, we set a maximum incoming water flow of 0.1113 m/s. The laminar velocity profiles are obtained by solving a system of equations,

$$\frac{\partial v_x}{\partial x} + \frac{\partial v_y}{\partial y} = 0,$$

$$v_x\frac{\partial v_x}{\partial x} + v_y\frac{\partial v_x}{\partial y} = -\frac{1}{\rho}\frac{\partial p}{\partial x} + \gamma\left(\frac{\partial^2 v_x}{\partial x^2} + \frac{\partial^2 v_x}{\partial y^2}\right),$$

$$v_x\frac{\partial v_y}{\partial x} + v_y\frac{\partial v_y}{\partial y} = -\frac{1}{\rho}\frac{\partial p}{\partial y} + \gamma\left(\frac{\partial^2 v_y}{\partial x^2} + \frac{\partial^2 v_y}{\partial y^2}\right),$$

where ρ is density, γ is kinematic viscosity and p is pressure. For the cases considered the resulted velocity profiles are presented in Figure 3. These velocity profiles are generated by *ANSYS 19.2*.

To test the effect of number of segment and interior collocation point to numerical solutions, the DRM is applied using different sets of number of element and interior collocation point to solve Case 1. There are four different sets of elements and interior collocation points, namely Set C, Set D, Set E, and Set F. In Set C, the number of element is 200 and the number of interior collocation point is 351. In Set D the number of element is 250 and the number of interior collocation point is 351. The numbers of element and interior collocation point in Case E are 200 and 423, respectively. In Set F the number of elements is 250 and the number of interior collocation points is 423. Some of numerical results obtained using these different sets of element and interior collocation points are summarized in Table II.

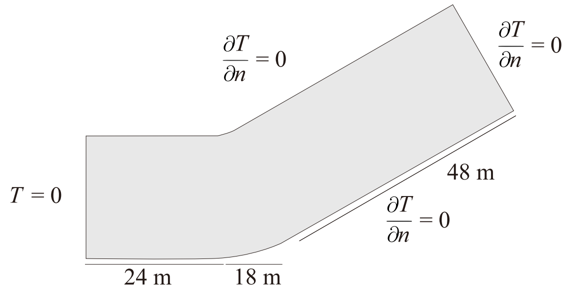

(a) Case 1

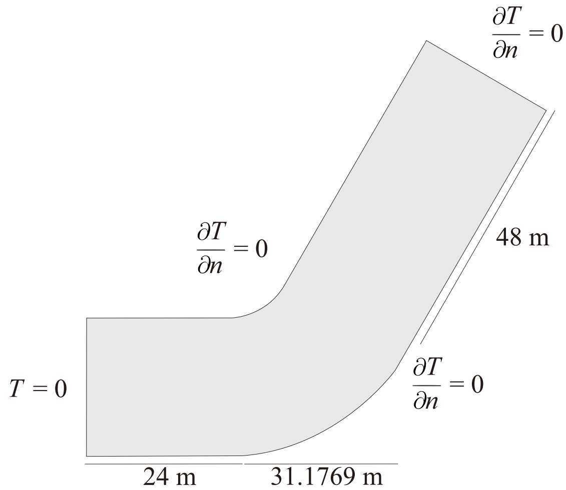

(b) Case 2

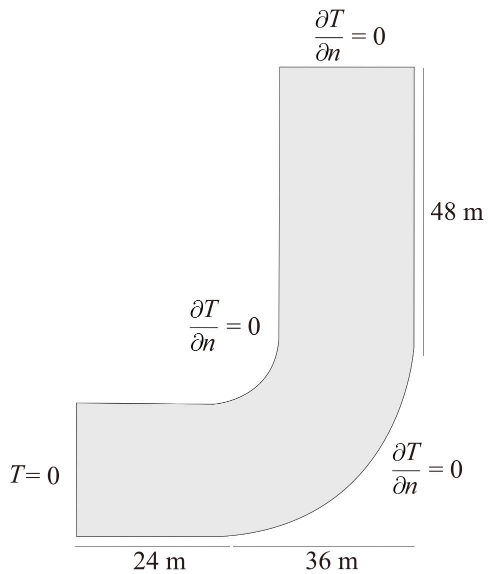

(c) Case 3

Fig. 2: Region and boundary conditions of steady pollutant concentration range for three different cases.

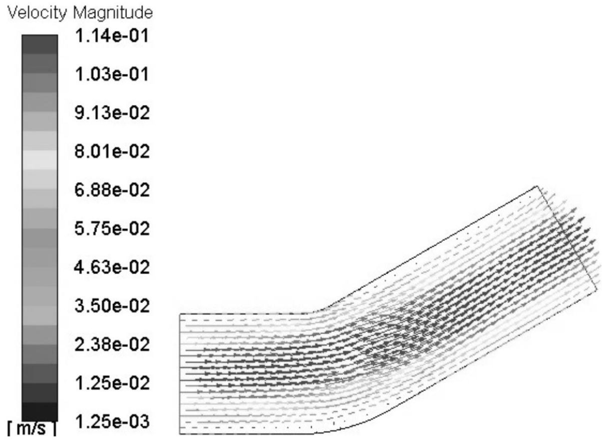

(a) Case 1

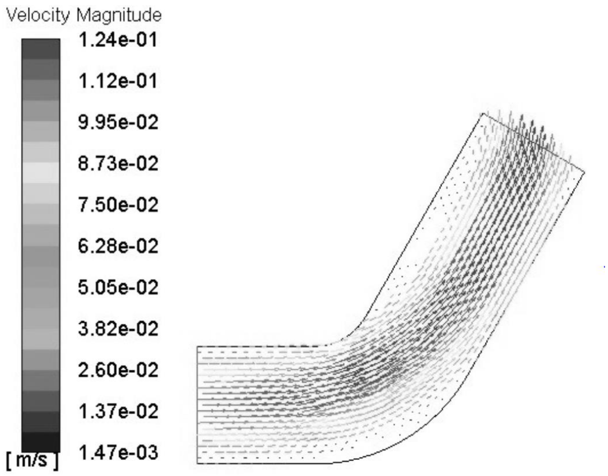

(b) Case 2

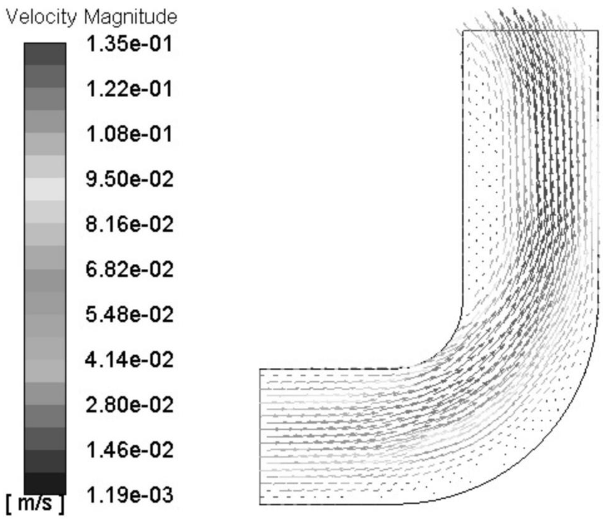

(c) Case 3

Fig. 3: Velocity profile for Case 1, Case 2, and Case 3, generated by *ANSYS 19.2*.

TABLE II: Numerical solutions at selected points for Case 1

Point	Set C	Set D	Set E	Set F
(12.00, 6.00)	0.076758	0.076495	0.076284	0.076114
(12.00, 12.00)	0.081824	0.081591	0.081406	0.081257
(12.00, 18.00)	0.089827	0.089584	0.089394	0.089242
(30.23, 6.65)	0.164204	0.163798	0.163476	0.163216
(28.98, 12.52)	0.173449	0.173077	0.172781	0.172543
(27.74, 18.39)	0.197025	0.196693	0.196430	0.196220
(70.67, 28.30)	0.242782	0.242189	0.241713	0.241330
(67.67, 33.50)	0.242923	0.242336	0.241865	0.241485
(64.67, 38.69)	0.242875	0.242292	0.241825	0.241447

In Table II, numerical solutions at nine different points obtained using Set A, Set B, Set C, and Set D are presented. It can be observed from Table II that at the same point, numerical solutions obtained from different sets of segment and interior collocation point are about the same. The differences between them are less than 0.0006. Hence, for further implementation of the DRM, we use Set C for solving the problems in Figure 2. Surface plots of the numerical results for Case 1, Case 2, and Case 3 are presented in Figure 4.

For further discussion, we analyze the behavior of the pollutant concentration values at lines l_1, l_2, and l_3 from three cases. Line l_1 is the line connecting point (24,24) and point (24,0). Line l_2 is the line in the middle of the curved fluid path forming an angle of $\theta/2$ with line l_1. Line l_3 is the line forming an angle of θ with line l_1. The illustration of these three lines can be seen in Figure 5. Numerical results obtained along these three lines are presented in Figure 6a, Figure 6b, and Figure 6c.

Pollutant concentrations along the three lines, l_1, l_2, and l_3, from Case 1, Case 2, and Case 3 are shown in Figure 6. In Figure 6(a), it can be seen that there is no significant effect between the magnitude of the inclination and the pollutant concentration value along line l_1. This means that before entering the curved path, pollutant concentration values are relatively the same for all cases. All cases have the same tendency that the value of pollutant concentration decreases monotonically along line l_1. The value of the pollutant concentration at point around the source point is about 0.262 gram/litre and at furthest point from the source point is about 0.139 gram/litre.

Figure 6b shows a comparison of the value of pollutant concentration along line l_2. As in Figure 6a, all cases have pollutant concentration value which is decreases monotonically along line l_2. Before reaching point which is 5.182 m from the source point, the higher the inclination, the lower the pollutant concentration value. After point which is 5.182 m from the source point, the higher the inclination, the higher the pollutant concentration value. The pollutant concentration at point around the source point has the highest value which is about 0.227 mg/litre and the lowest value which is about 0.206 mg/litre. The pollutant concentration at farthest point from the source point has the highest value which is about 0.191 mg/litre and the lowest value which is about 0.166 mg/litre. The changes in the concentration values of all cases will be stable after point which is 20.727 m from the source point.

Figure 6c shows a comparison of the value of pollutant concentration along line l_3. It can be seen that only in Case 1 the pollutant concentration value decreases monotonically and in Case 2 tends to be stable along line l_3. The pollutant

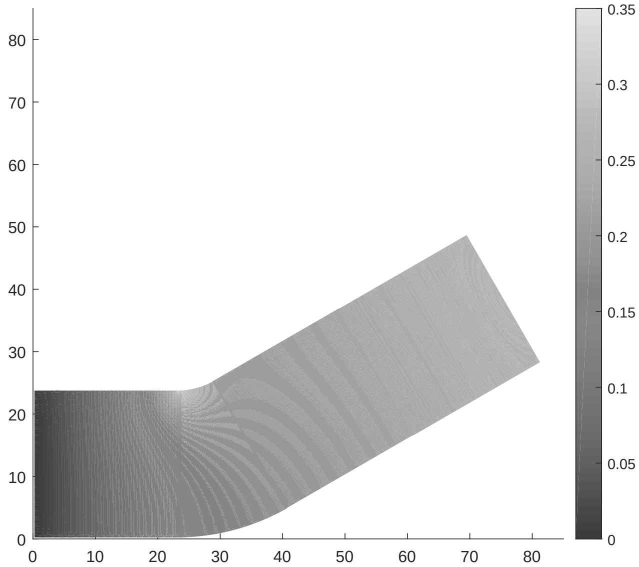

(a) Case 1

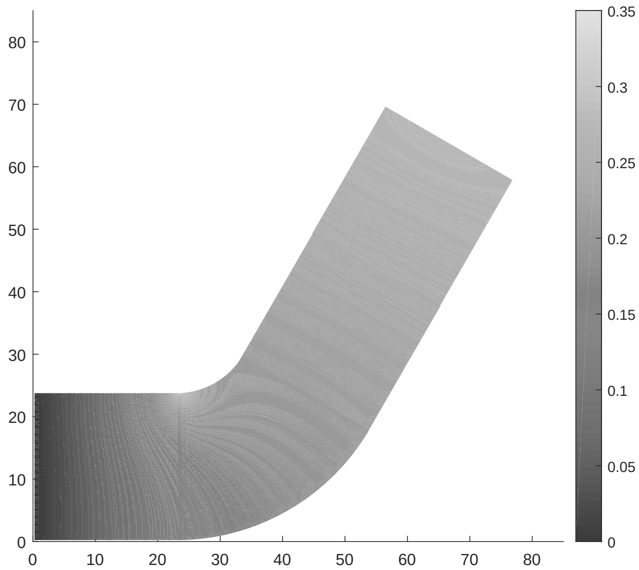

(b) Case 2

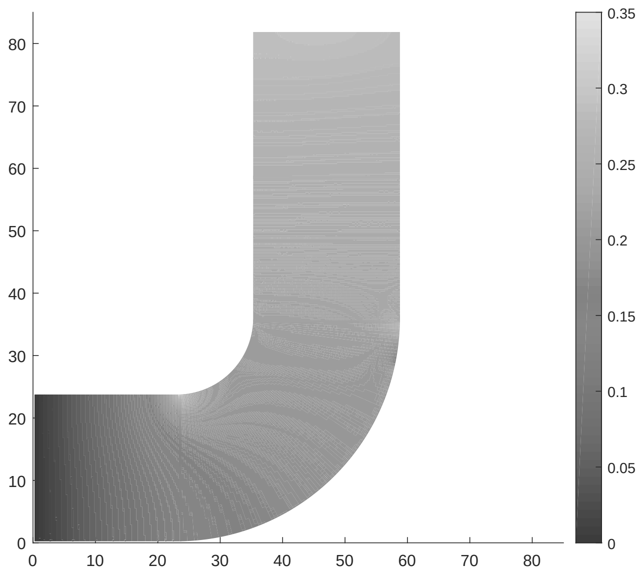

(c) Case 3

Fig. 4: Surface plot of pollutant concentration for Case 1, Case 2, and Case 3.

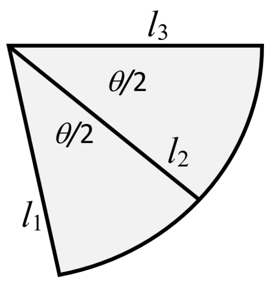

Fig. 5: Line l_1, l_2, and l_3 formulation

concentration at point around the source point has the highest value which is about 0.218 mg/litre in Case 3 and the lowest value which is about 0.209 mg/litre in Case 2. The pollutant concentration at furthest point from the source point has the highest value which is about 0.239 mg/litre in Case 3 and the lowest value which is about 0.185 mg/litre in Case 1. This means that before exiting the curved path, the pollutant concentration value at furthest point from the source point will be higher when the higher the inclination.

For further discussion, we test the effect of the flow velocity and the source value to the values of pollutant concentration along l_1, l_2, and l_3 for Case 1. We consider three different values of flow velocity. The flow velocities considered are 0.0557 m/s, 0.1113 m/s, and 0.2226 m/s. Numerical results obtained using these three flow velocities are presented in Figures 7a - 7c. We also consider three different values of source. The values of source are 0.9345 gram/second, 1.8691 gram/second, and 3.7382 gram/second. Numerical results obtained are presented in Figures 8a - 8c.

Figure 7 shows the concentrations distribution of pollutant which is influenced by the magnitude of the incoming velocity. It can be seen that the higher the velocity the lower the pollutant concentration. It can also be seen that all graphs have a monotonous descending behavior. Along l_1, the differences in pollutant concentration get higher as the distance from upper point bigger. Along l_2 and l_3, the differences in pollutant concentration are about the same.

Figure 8 shows the distributions of pollutant concentration influenced by the value or the intensity of the pollutant source (Q). From the figures, it can seen that at the same line, the trends of pollutant distribution resulted from different values of pollutant are about the same. It can be observed that the higher the source value the higher the pollutant concentration, which is expected. It can also be observed that lower source value results in less variation in pollutant concentration.

Figure 9 shows the distribution of pollutant concentrations which are influenced by locations of the pollutant source. Here the pollutant sources are selected at points (24,24) and (24,0), which are denoted by Q_A and Q_B, respectively. Unlike the previous graphs, the fashions of the distribution of pollutant concentrations values with pollutant source at Q_B is inversely proportional to those resulted from source at Q_A. It can be observed that concentration of pollutant for the two different source locations is the same at position about 11.999 m on line l_1, about 14.181 m on line l_2, and

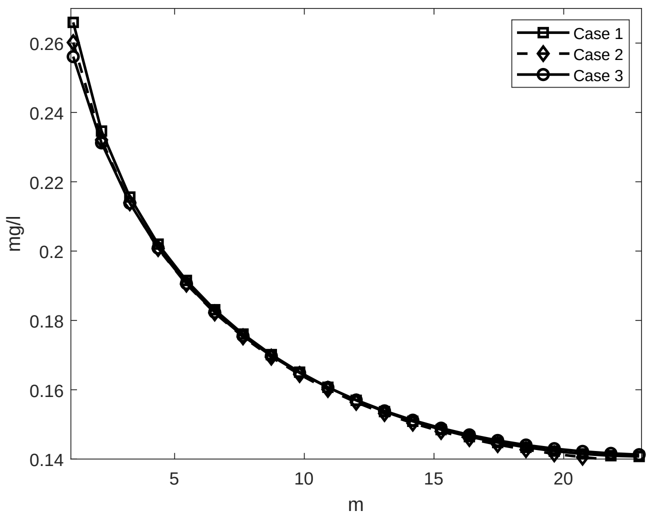

(a) Along line l_1

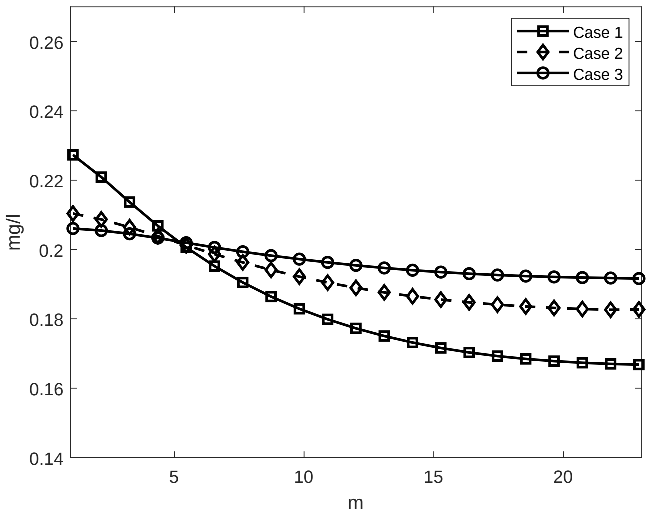

(b) Along line l_2

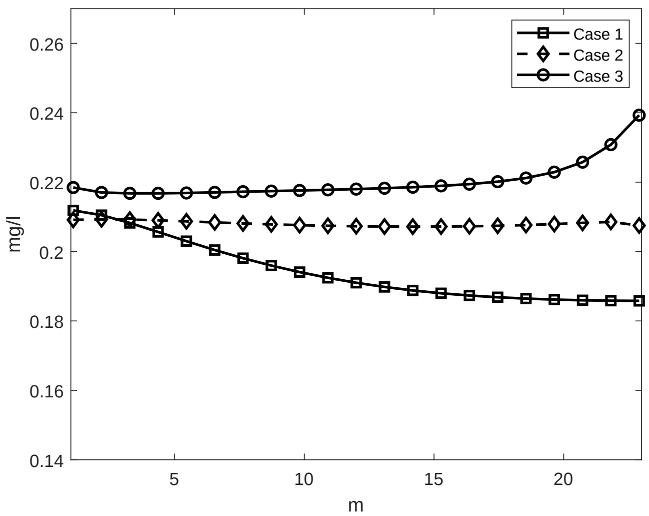

(c) Along line l_3

Fig. 6: Pollutant concentration along three lines for Case 1, Case 2, and Case 3.

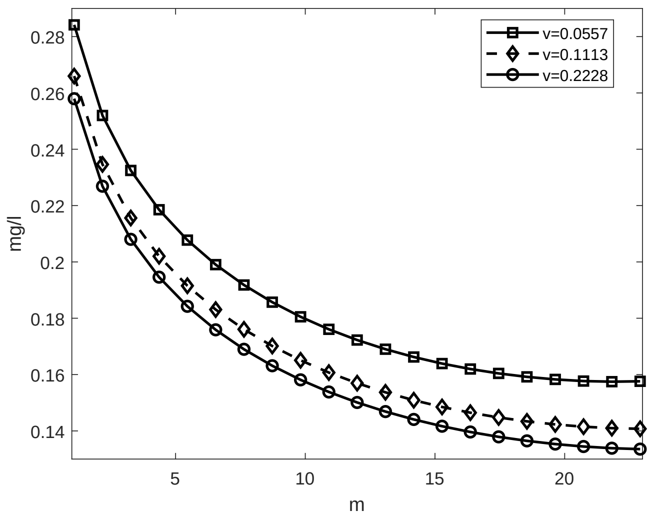

(a) Along line l_1.

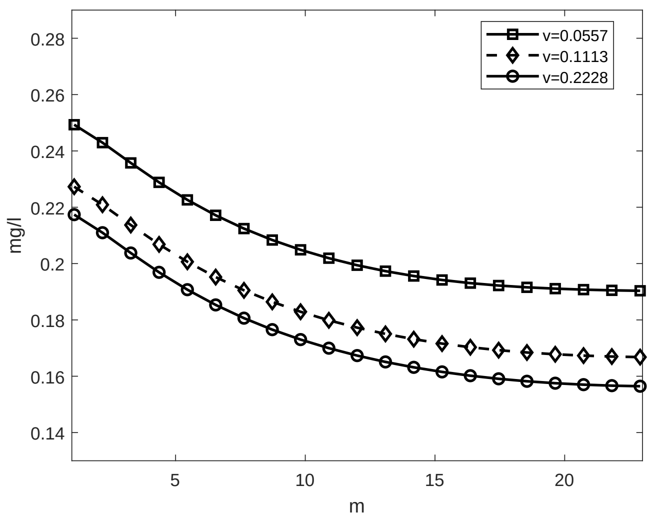

(b) Along line l_2.

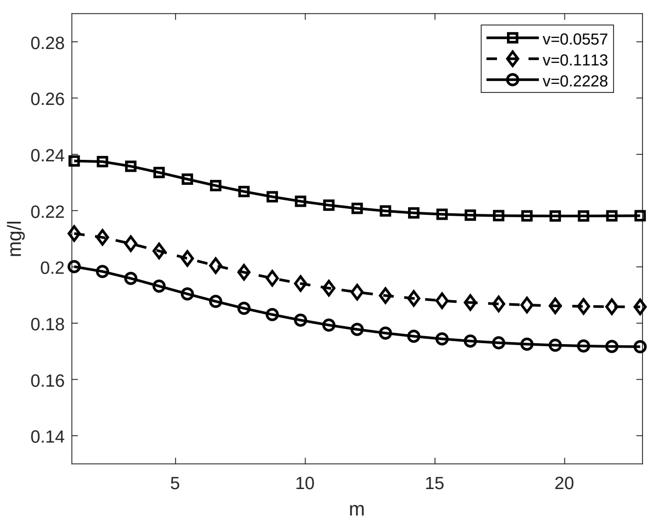

(c) Along line l_3.

Fig. 7: Pollutant concentration along lines l_1, l_2, and l_3 based on incoming velocity

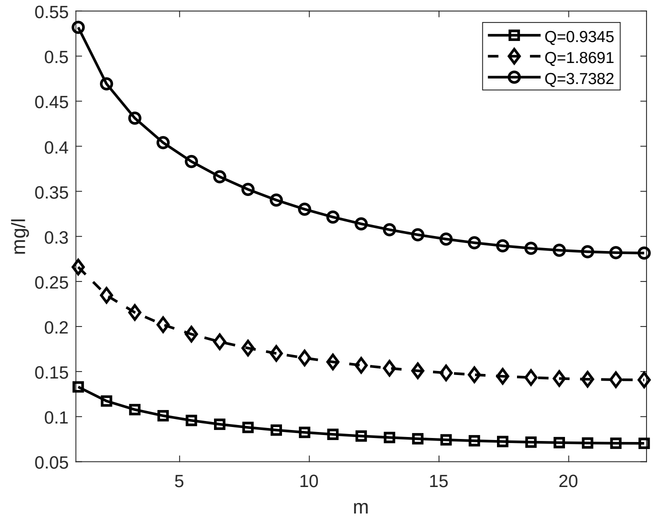

(a) Along line l_1.

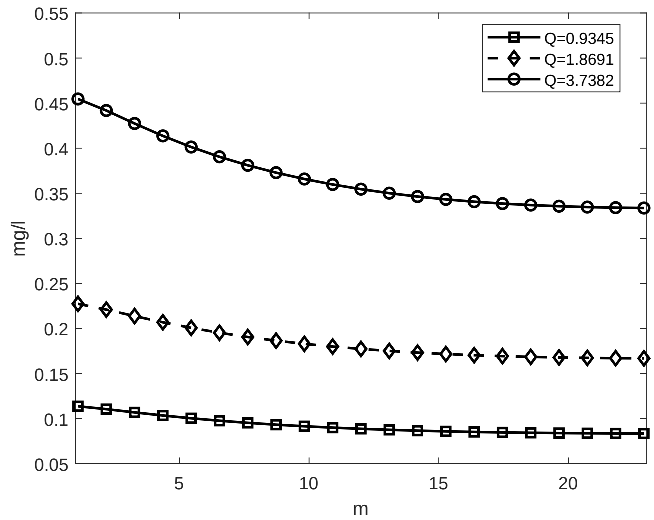

(b) Along line l_2.

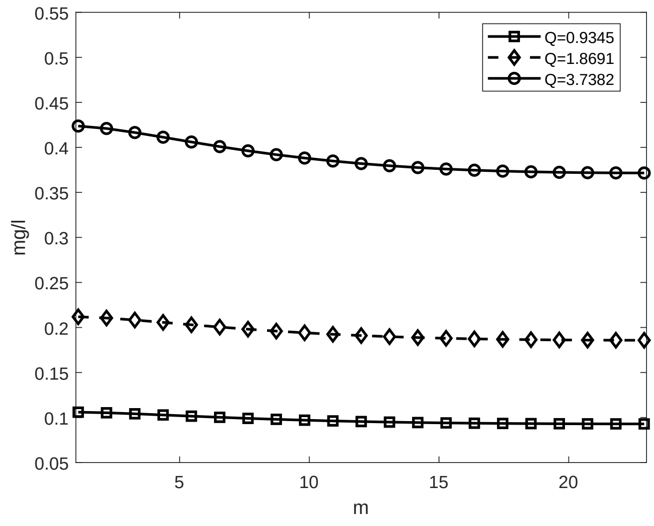

(c) Along line l_3.

Fig. 8: Pollutant concentration along lines l_1, l_2, and l_3 with different values of source intensity

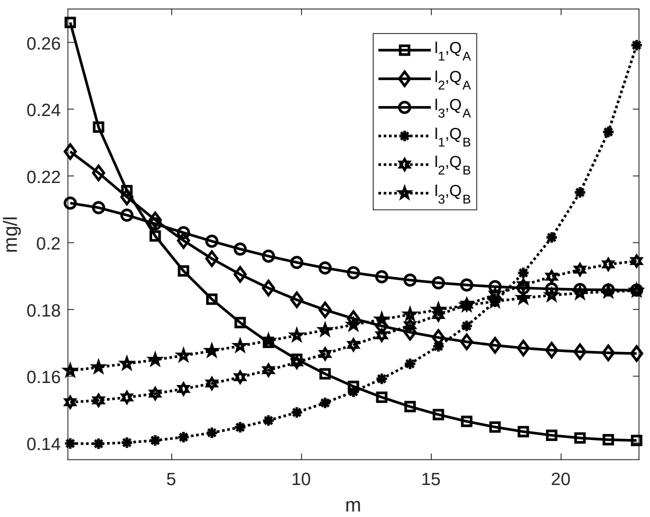

Fig. 9: Pollutant concentration along line l_1 based on source position

about 23.272 m on line l_3.

From the figure it seems that the total pollutant concentration resulted from the source at Q_A is different from that resulted from Q_B. To compute the total pollutant concentration along lines l_1, l_2, and l_3, we compute

$$\int_{l_i} T(x,y)ds,\ i = 1, 2, 3, \tag{8}$$

using Simpson's rule. It is assumed that the volume of water along each line is 240 litres. The results obtained using the Simpson's rule are presented in Table III.

TABLE III: Total Pollutant in 240 litres water.

Source	Along l_1	Along l_2	Along l_3
Q_A	41.2549 mg	44.4622 mg	46.7023 mg
Q_B	40.8488 mg	41.1404 mg	41.9351 mg

From Table III, it can be seen that among the three lines, the highest amount of pollutant is at line l_3, and the lowest amount is at l_1. It can also be seen that for Q_A, there are significant increases in the total amount of pollutant from 41.2549 mg along l_1 to 44.4622 mg along l_2, and from 44.4622 mg along l_2 to 46.7023 mg along l_3. The increases are about 3.2073 mg and 2.2401 mg, respectively. On the other hand, Q_B results in insignificant increases in the total amount of pollutant. The increases are about 0.2916 mg and 0.7947 mg, respectively, which are much smaller than those resulted from Q_A. From these results, it seems that pollutant source placed at Q_A results in higher amount of pollutant than that placed at Q_B.

IV. Concluding remarks

A mathematical model for steady pollutant concentration range in twinned fluid path with laminar water flow has been constructed. The model has been successfully solved numerically using a DRM. This method is tested to solve problem with analytical solution and problems without analytical solution. The problem without analytical solution is the problem involving steady pollutant concentration range in twinned fluid path with inclinations of 30^o, 60^o, and 90^o.

To investigate the accuracy of numerical solution using DRM, Set A and Set B are applied to the problem with analytical solution. In Set A, the number of elements is 80 and the number of interior collocation points is 81. In Set B, the number of segments is 200 and the number of interior collocation points is 196. It seems that the absolute errors of the numerical solutions obtained using Set A and Set B are less than 0.0006 and 0.0002, respectively. It can also be seen that Set B results in better accuracy than Set A. This means that generally the higher the number of segments and interior colllocation points the more accurate the numerical solution obtained.

From the previous discussion, it can be concluded that before entering the curved path, the pollutant concentration value is relatively the same and decreases monotonically. At the middle of the curved path, all cases have pollutant concentration values which is also decreases monotonically. The higher the inclination, the higher the pollutant concentration value after a point with distance of 5.182 m from the source point. It can also be concluded that before leaving the curved path, the higher pollutant concentration at furthest point from the point source occurs in the path with higher inclination.

From a deeper discussion for Case 1 by considering the influence of the intensity of the incoming velocity, the intensity of the pollutant source and positions of the pollutant source. It may be concluded that the higher the value of the incoming velocity, the lower the values of the pollutant concentrations, and two positions of the selected pollutant source produce the analogous pollutant concentrations distribution.

Moreover, position of source affects the concentration of pollutants. Distribution of pollutant concentration influenced by source point at Q_B is inversely proportional to that influenced by source point at Q_B. From the results presented, it can be concluded that total pollutant resulted from Q_A is higher than that resulted from Q_B.

References

[1] N. Samec and L. Skerget, *Numerical modelling of pollutant dispersion in water systems*, vol 25. Slovenia: WIT Press, 1998.

[2] A. D. Polyanin, "Functional separable solutions of nonlinear convection–diffusion equations with variable coefficients Author links open overlay panel," Communications in Nonlinear Science and Numerical Simulation, Vol. 73, pp. 379 - 390, 2019.

[3] V. F. Morales-Delgadoa, J. F. Gomez-Aguilar and M. A. Taneco-Hernandez, "Analytical solution of the time fractional diffusion equation and fractional convection-diffusion equation," Revista Mexicana de Fisica, Vol. 65, pp. 82 – 88, 2019.

[4] W. Fajie, F. Chia-Ming, Z. Chuanzeng and L. Ji," A Localized Space-Time Method of Fundamental Solutions for Diffusion and Convection-Diffusion Problems," Adv. Appl. Math. Mech., Vol. 12(4), pp. 940 - 958, 2020.

[5] Y. Xingxing, W. Fajie, H. Qingsong and Q. Xiang-Yun, "A novel space–time meshless method for nonhomogeneous convection–diffusion equations with variable coefficients," Applied Mathematics Letters, Vol. 92, pp. 144 - 150, 2019.

[6] Z. Mengxin, Z. Weifeng and L. Ping, "Lattice Boltzmann method for general convection-diffusion equations: MRT model and boundary schemes," Journal of Computational Physics, Vol. 389, pp. 147 - 163, 2019.

[7] H. Ji-Huan, "A simple approach to one-dimensional convection-diffusion equation and its fractional modification for E reaction arising in rotating disk electrodes," Journal of Electroanalytical Chemistry, Vol. 854, p. 113565, 2019.

[8] D. Clements and M. Lobo, "A BEM for Time Dependent Infiltration from an Irrigation Channel," Engineering Analysis with Boundary Elements 2010, vol. 34, pp. 1100 - 1104, 2010.

[9] I. Solekhudin and K.C. Ang, "A Laplace Transform DRBEM with a Predictor-Corrector Scheme for Time Dependent Infiltration from Periodic Channels with Root Water Uptake," Engineering Analysis with Boundary Elements, vol. 50, pp. 141 - 147, 2015.

[10] I. Solekhudin, "A Numerical Method for Time-Dependent Infiltration from Periodic Trapezoidal Channels with Different Types of Root-Water Uptake," IAENG International Journal of Applied Mathematics, vol. 48, no. 1, pp. 84 - 89, 2018.

[11] Munadi, I. Solekhudin, Sumardi, and A. Zulijanto, "A Numerical Study of Steady Infiltration from a Single Irrigation Channel with an Impermeable Soil Layer," Engineering Letters, vol. 28, no. 3, pp. 643 - 650, 2020.

[12] B.I. Yun and W.T. Ang, "A Dual Reciprocity Element Approach for Axisymmetric Nonlinear Time-Dependent Heat Conducyion in a Non-homogeneous Solid," Engineering Analysis with Boundary Elements, vol. 34, no. 8, pp. 697 - 706, 2010.

[13] N.Y. Ashar, *An Application of Dual Reciprocity Boundary Element Method on Calculation of Pollutant Concentration Range in Twinned Path with Laminar Water Flow*, M.Sc. Thesis, Department of Mathematics, Universitas Gadjah Mada, 2020.